Hindawi Publishing Corporation
Journal of Combustion
Volume 2012, Article ID 918754, 8 pages
doi:10.1155/2012/918754

Research Article

Moving Bed Gasification of Low Rank Alaska Coal

Mandar Kulkarni[1] **and Rajive Ganguli**[2]

[1] *Department of Petroleum Engineering, University of Alaska Fairbanks, Fairbanks, AK 99775, USA*
[2] *Mineral Industry Research Laboratory, University of Alaska Fairbanks, Fairbanks, AK 99775, USA*

Correspondence should be addressed to Rajive Ganguli, rganguli@alaska.edu

Received 7 July 2012; Revised 4 October 2012; Accepted 4 October 2012

Academic Editor: Eliseo Ranzi

This paper presents process simulation of moving bed gasifier using low rank, subbituminous Usibelli coal from Alaska. All the processes occurring in a moving bed gasifier, drying, devolatilization, gasification, and combustion, are included in this model. The model, developed in Aspen Plus, is used to predict the effect of various operating parameters including pressure, oxygen to coal, and steam to coal ratio on the product gas composition. The results obtained from the simulation were compared with experimental data in the literature. The predicted composition of the product gas was in general agreement with the established results. Carbon conversion increased with increasing oxygen-coal ratio and decreased with increasing steam-coal ratio. Steam to coal ratio and oxygen to coal ratios impacted produced syngas composition, while pressure did not have a large impact on the product syngas composition. A nonslagging moving bed gasifier would have to be limited to an oxygen-coal ratio of 0.26 to operate below the ash softening temperature. Slagging moving bed gasifiers, not limited by operating temperature, could achieve carbon conversion efficiency of 99.5% at oxygen-coal ratio of 0.33. The model is useful for predicting performance of the Usibelli coal in a moving bed gasifier using different operating parameters.

1. Introduction

Gasification is considered to be one of the most efficient technologies to convert raw, low-cost coal into clean and highly priced chemicals, fuels, and power. Therefore, as energy prices continue to fluctuate and/or rise, gasification is often brought up as an alternate source of energy and chemicals. The massive coal reserves of Alaska [1] make it a good location for exploiting the technology for energy and chemicals. Chaney and Sheets [2] studied the feasibility of using coal gasification for power generation and chemical byproducts. The plant was to be located in the Cook Inlet region of Alaska and would use coal from the nearby Beluga coal fields (mine permit process underway). The intent of the study was to look at modifying the feedstock of a local fertilizer plant from natural gas to coal, while generating power at the same time. In a similar study, Bibber et al. [3] studied the gasification of the low-rank Usibelli coal for producing Fischer-Tropsch liquids. In both cases, only entrained flow and fluidized bed gasifiers were studied, leaving out moving bed gasifiers. Therefore, the primary objective of this research work was to evaluate performance of Usibelli coal in a moving bed gasifier.

1.1. Moving Bed Gasifier. In a moving bed gasifier, coal flows downward due to gravity in a countercurrent fashion to the gasifying agents, air, steam, and product gases. Moving bed gasifier is usually operated below the ash fusion temperature to avoid clinkering of the coal. Usually noncaking coals are preferred [4]. Coal sized in a particle size range from 6.35 mm to 38.1 mm is fed from the top of the reactor, while steam and oxygen are blown from the bottom of the reactor. Countercurrent flow of the coal renders excellent thermal efficiency because of the fact that the most of the heat generated in the reactor is utilized in the reactor itself. As the coal flows downward, it undergoes a series of different reactions that include drying, devolatalization, gasification, and combustion. These are described next.

1.1.1. Drying. Drying is the first process that coal undergoes during its countercurrent flow in a moving bed reactor.

During this process, the hot upward-flowing gases in the reactor remove the moisture inside the coal. The temperature maintained in the drying section is usually below 300°C depending on the moisture content of the coal.

1.1.2. Devolatalization. Devolatalization is the next step in moving bed gasifier. It is a process in which coal is transformed at elevated temperatures to produce gases, tar, and char [5]. Devolatalization step in a moving bed gasifier determines the composition of tars in the product gas. The composition of tars, char, and product gases after a devolatalization process largely depends on the coal type, temperature, heating rate, and pressure. Low rank coal has relatively larger percentages of volatile matter and release large amount of light gases and less amount of tar as compared to higher rank coals [6]. Suuberg et al. [7] studied the effect of temperature on the volatile yield during the coal pyrolysis. He concluded that the yields of the volatiles increase exponentially with the temperature. He also investigated the effect of pressure on the composition of product gases. Vacuum pyrolysis of coal produces higher yields of heavy hydrocarbons and lower yields of light gases than are obtained at atmospheric conditions. Gibbins-Matham and Kandiyoti [8] found increase in volatile yield in three of the four coals tested when the heating rate was increased from 1 K/s to 1000 K/s. For Pittsburgh no. 8 coal, one of the three coals that saw an increase in volatile yield, he concluded that the increase was mainly due to increase in tar production at higher heating rate. Larger particle size tends to slow down heat and mass transfer rates and reduce the overall reaction rates and affecte the quantity and quality of the product gases [9].

1.1.3. Char Gasification and Combustion. The gasification and combustion of char involves series of heterogeneous reactions with oxygen and steam that are responsible for autothermic nature of the gasification process. The following reactions occur during this stage [10].

Char-Oxygen reaction:

$$C + \frac{z+2}{2z+2}O_2 \longrightarrow \frac{z}{z+1}CO + \frac{1}{z+1}CO_2 \quad +111\,\text{KJ/mol} \tag{1}$$

Char gasification reaction:

$$C + H_2O \longrightarrow CO + H_2 \quad -131.3\,\text{KJ/mol} \tag{2}$$

Boudouard reaction:

$$C + CO_2 \longrightarrow 2CO \quad -172.8\,\text{KJ/mol} \tag{3}$$

Methanation reaction:

$$C + 2H_2 \longrightarrow CH_4 \quad +75\,\text{KJ/mol} \tag{4}$$

Water-gas shift reaction:

$$CO + H_2O \longrightarrow CO_2 + H_2 \quad +141.1\,\text{KJ/mol} \tag{5}$$

Hydrogen oxidation:

$$H_2 + 0.5O_2 \longrightarrow H_2O \quad +242\,\text{KJ/mol}, \tag{6}$$

where z: ratio of CO, and CO_2 mean concentrations = 2500 $\exp(-6249/T)$. Kinetics expression for all these reactions has been adopted from [10, 11].

The higher residence time and counter current flow in moving bed gasifier favor higher carbon conversion as compared to fluidized bed and entrained flow gasifiers. The product gas contains significant amount of other byproducts like tars, phenols, and ammonia which requires vigorous cleaning. Oxygen or air requirements are lower than that for fluidized bed and entrained bed. Moving bed gasifier is suitable for low-rank coals especially those with higher percentage of moisture.

2. Model Description

The Aspen Plus simulation model by [12] was the foundation for the model used in the research. The model process flow sheet is shown in Figure 1.

The following were modified from [12].

(i) Component attributes and heating value of feed coal.
(ii) Yield of pyrolysis gases, tars, and char in devolatalization step.
(iii) Operational parameters that include coal, steam and oxygen flow rate, pressure, and temperature.
(iv) Gasifier operational conditions that includes gasifier height, diameter, and pressure.
(v) FORTRAN code to reflect the kinetics of the reactions.

The various Aspen reactor blocks used in the process flow sheet are described in Table 2. Table 3 lists the properties of Usibelli coal. All the processes occurring in the gasifier, that is, drying, pyrolysis, gasification, and combustion are included in the model. Developing Aspen Plus model requires knowledge of reaction stoichiometry, reaction rates, kinetics, mass, and heat transfer. The model was used to predict the composition of product gas, temperature profile, and effect of process variables on the syngas composition [12].

Assumptions in the model were as follows.

1. The model is in steady state.
2. Coal and gas flow as plug flow. Plug flow assumes constant velocity across the cross section of the gasifier with no backmixing.
3. Residence time of the coal in drying and pyrolysis section is assumed to be negligible as compared to combustion-gasification section.
4. The pressure drop in the gasifier is neglected.
5. Volumetric reaction represents all gas-solid reactions except char combustion which is according to shrinking core model.
6. Gas temperature is the same as solid temperature at every point in the gasifier.

The various processes are modeled as follows.

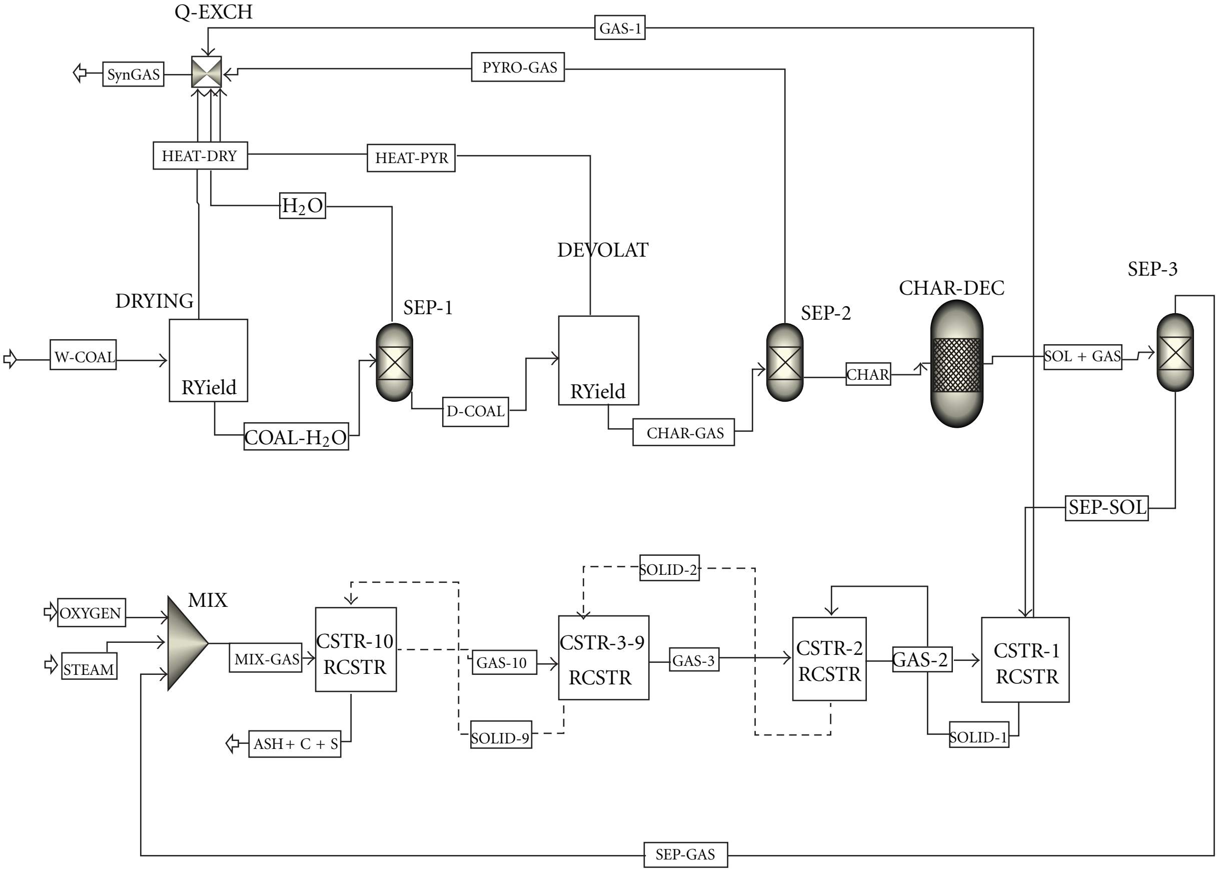

Figure 1: The process flow sheet (modified version of [12]) for the simulation model.

Coal Drying. The wet coal (W-COAL) is first fed to the R-Yield DRYING block which is used to simulate the drying reaction occurring at the top of the gasifier. In this block, moisture content inside the wet coal is driven off. The amount of water that vaporizes depends upon the moisture content specified in the proximate analysis of the wet coal. In the Usibelli coal case, moisture content of the wet coal is 27%. Thus,

$$\begin{aligned}&\text{the yield of the water vapor in RYield block}\\&\quad = 0.27 * \text{mass of wet coal}, \qquad (7)\\&\text{the yield of the dried coal} = 0.73 * \text{Mass of wet coal}.\end{aligned}$$

The heat required for the drying reaction is supplied by the hot gases leaving from combustion and gasification section of the reactor. Water vapor (H_2O) and dried coal (D-COAL) are separated in Sep-1 block.

Coal Devolatalization. The dried coal is then sent to DEVOLAT block which simulates the devolatalization of the dried coal using RYield reactor model. In the DEVOLAT block, most of the volatile matter inside the dried coal is converted to volatile products. The products from this block include CO, H_2, CO_2, H_2O, CH_4, Tar, C_2H_4, ash, and char. The yield of the different products is based on the results obtained from the Suuberg et al. [7]. The ultimate analysis of the coal that is used in [7] closely matches with the Usibelli coal. The only small difference lies in the fact that Usibelli coal has negligible amount of sulfur, while [7] has around 1.18%. The proximate and ultimate analysis of the char after the pyrolysis of the Usibelli coal is obtained from the work done by [13] on the characterization of coal products from high Temperature processing of Usibelli low-rank coal. Char (CHAR) and Pyrolysis products (PYRO-GAS) are then separated in SEP-2 separator.

Char Gasification and Combustion. The ungasified char that remains after pyrolysis is then sent to CHAR-DEC block modeled by RStoic reactor. Based on the ultimate analysis of the char, it is decomposed into its constituent specified by the following reaction:

$$\text{CHAR} \longrightarrow C_{\text{solid}} + H_2 + N_2 + S_{\text{solid}} + \text{ASH} + O_2 \qquad (8)$$

As the moving bed gasifier is a counter-current reactor, there is a need to design a model which will incorporate counter-current flow of solid components and the gases in char gasification and combustion section. The drying and pyrolysis are considered to occur instantaneously as compared to gasification and combustion.

In this model, the counter current flow is accomplished by a series of RSCTR reactors models. The criterion for selecting the number of RCSTR reactors for gasification and combustion section was based on the carbon conversion. It was found to be maximum when 10 RCSTR reactors were used in series [12].

After the decomposition of the char in CHAR-DEC block, solid components of the char, $C_{(solid)}$ and $S_{(solid)}$, and ash are separated from the gaseous components H_2, O_2, and N_2. Solid components are sent to CSTR-1, while gases are sent to the CSTR-10 along with oxygen and steam feed.

The solid components move from CSTR-1 to CSTR-2 to CSTR-3, and so forth, all the way down to CSTR-10, while the gaseous components, reflecting counter current flow, move up from CSTR-10 to CSTR-9, and so forth, all the way up to CSTR-1. The final gases leaving from CSTR-1 are then mixed with pyrolysis gas, and drying gas streams, while solids (ash + S + C) are separated from the bottom of the CSTR-10. The heat associated with combustion and gasification gas is used in drying and devolatalization process. The reaction kinetics for all the reactions that are occurring in gasifier is written in a separate FORTRAN code that is a special feature Aspen Plus.

For the heterogeneous char-oxygen reaction (1), unreacted core shrinking core model has been applied for the determination of the reaction rate as it is necessary to consider diffusion of the oxygen inside the coal diameter which is the slowest and rate limiting step [10].

$$\text{Rate} = R_1 = \frac{1}{1/k_{\text{film}} + 1/k_s Y^2 + 1/k_{\text{ash}}} \left(P_i - P_i{}^*\right), \tag{9}$$

where k_{film} is the mass transfer coefficient for gas film diffusion, k_{ash} is the mass transfer coefficient for ash diffusion, k_s is the chemical reaction constant, P_i is the partial pressure of reactant i, and $P_i{}^*$ is the back reaction equilibrium pressure of reactant i. Y is the ratio of radius of unreacted core to the radius of feed coal particle. For reaction (1), burning of the char particles occurs so fast at the surface that makes gas film diffusion and ash film diffusion rate controlling steps. So (9) reduces to

$$R_1 = \frac{1}{1/k_{\text{film}} + 1/k_{\text{ash}}} \left(P_i - P_i{}^*\right). \tag{10}$$

The expression for k_{film}, k_{ash} for reaction (1), and rate equation for reaction (2), (3), (4), (5), and (6) have been adopted from Wen's model for moving bed gasifier [10, 11] and are shown in Table 1.

Heat Balance in the Gasifier. Energy in the gasifier is generated due to higher heating value of coal and exothermic nature of the reactions (1), (4), (5), and (6).

The Energy balance in the gasifier is given by following equation:

$$\begin{aligned}
&\text{Heating value of coal} \\
&\quad + \text{enthalpy in with } [\text{Coal} + \text{steam} + \text{oxygen}] \\
&\quad = \text{heating value of product gases} \\
&\quad + \text{enthalpy out with } [\text{Product gases} + \text{tars} \\
&\quad + \text{product char}] + \text{heat losses in the reactor.}
\end{aligned} \tag{11}$$

Heat losses in the reactor are composed of endothermic heats of reaction and heat losses to the surrounding environment through the reactor walls. Heat losses to the surrounding environment through the reactor wall are considered zero in this work.

Aspen Plus contains all the physical and chemical properties of the gases and solids with the exception of coal. In Aspen Plus, heating value and enthalpy of coal are calculated using HCOALGEN model. This model includes a number of correlations for heat of combustion, heat of formation, and heat capacity. Heat of combustion of coal can be calculated using different correlations such as Boie correlation, Dulong correlation, and Grummel and Davis correlation.

Boie Correlation. One has

$$\begin{aligned}
\text{Enthalpy of coal} = {} & 151.2\,\mathrm{C} + 499.77\,\mathrm{H} + 45.0\,\mathrm{S} \\
& - 47.7\,(\mathrm{O}) + 27.0\,\mathrm{N},
\end{aligned} \tag{12}$$

where C, H, S, O, and N represent weight fractions of carbon, hydrogen, sulfur, oxygen, and nitrogen, respectively, inside the coal which are taken from the ultimate analysis of the dry mineral matter free coal.

The more detailed energy balance in the gasifier has been explained in [10]. The governing equation which was developed considering convective, radioactive, and conductive heat transfer and the heat of reactions is

$$\begin{aligned}
C_{\rho s} * \rho_s * \frac{dT}{dt} = {} & \frac{3}{r_o} * hc(T_w - T) + \frac{3\sigma Fe}{r_o}\left(T_w{}^4 - T^4\right) \\
& + \frac{3km}{r_o{}^2}(Tw - T) + \sum H_i r_i.
\end{aligned} \tag{13}$$

The important assumption in the simulation is that the solid and gas temperature are same at every location in the gasifier.

3. Model Validation

As experimental results on moving bed gasifier are not available for Usibelli sub-bituminous coal, the simulation results are compared with the experimental results obtained by [10] on Rosebud sub-bituminous coal, a coal similar in nature to the Usibelli coal. The model utilized identical operating parameters (shown in Table 4) as the experiments in [10]. Table 5 compares of product gas composition of the simulation model with the experimental data. The experiments by [10], however, reached a temperature of only 1000°C, as against 1182°C in the simulation. The model results are in close agreement with experimental results with the exception of H_2, CH_4, and tar composition. The small discrepancies with H_2 and CH_4 composition can be attributed to the fact that the highest temperature attained in the simulation was 1182°C, while in the experimental results, it was around 1000°C. Higher temperature favors the formation of H_2 and hinders the formation of CH_4 [14, 15]. The difference in tar yield is explained by the difference between the pyrolysis tar yields in [7] (used in the simulation) and that observed by [10].

Table 1: Rate expression for reactions occurring in char combustion gasification section [10].

Reaction	Rate expression
(1)	$R_1 = \dfrac{P_{O_2}}{1/k_{\text{film}} + 1/k_{\text{ash}}}$ $k_{\text{film}} = \dfrac{0.292 * 4.26 * [T/1800]^{1.75}}{d_p * T}$ $k_{\text{ash}} = k_{\text{film}} * \left[\dfrac{Y}{1-Y}\right] * \left[\varepsilon_p\right]^{2.5}$
(2)	$R_2 = k_2 * \exp(-E_2/RT)(P_{H_2O} - P_{H_2O}{}^*)[C]$ $P_{H_2O}{}^* = \dfrac{P_{H_2} * P_{CO}}{\exp(17.29 - 16330/T)}$
(3)	$R_3 = k_3 * \exp(-E_3/RT) * [C] * (P_{CO_2} - P_{CO_2}{}^*)$ $P_{CO_2}{}^* = P_{CO_2}/\exp(20.92 - 20280/T)$
(4)	$R_4 = \exp(-7.087 - 8078/T) * (P_{H_2} - P_{H_2}{}^*)[C]$ $P_{H_2}{}^* = \left[P_{CH_4}/\exp(-13.43 + 10100/T)^{0.5}\right]$
(5)	$R_5 = b * 2.877 * 10^5 * \exp(-27760/RT)$ $* \left(X_{CO}X_{H_2O} - \dfrac{X_{CO_2}X_{H_2}}{k_{\text{wgs}}}\right) X_{\text{ash}} * \rho_c$ $* P^{(0.5-P/250)} * (1 - \varepsilon_{\text{bed}}) * \exp(-8.91 + 5553/T)$ $k_{\text{wgs}} = \exp(-3.6890 + 7234/1.8T)$
(6)	$R_6 = 3 * 10^{10} * \exp(-16000/RT) *$ $(T * P_{O_2}/82.06)^{0.3} * (T * P_{H_2}/82.06)^{0.5} * \varepsilon_{\text{bed}}$

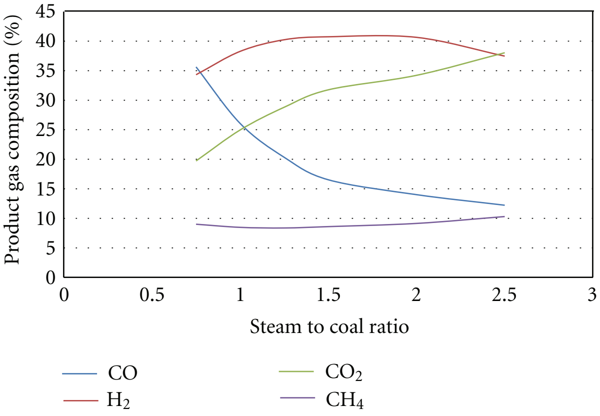

Figure 2: Effect of steam to coal ratio on product gas composition.

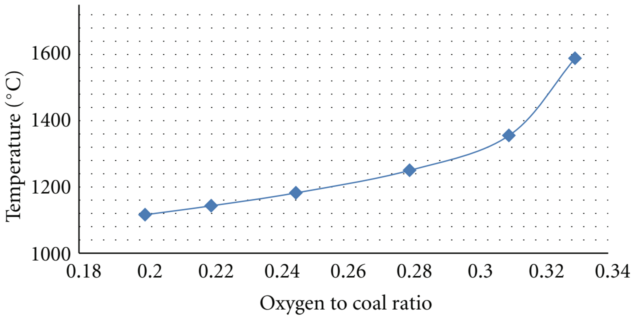

Figure 3: Effect of oxygen to coal ratio on gasifier temperature.

4. Impact of Operational Conditions

4.1. Effect of Steam to Coal Ratio. Steam to coal ratio was varied from 0.75 to 2.5 to see its effect on the performance of the gasifier. It was observed that as the steam flow rate increases, CO composition starts to decrease while methane and CO_2 start to increase (Figure 2). H_2 composition increases initially and then decreases as the temperature falls with increasing steam rate. It can be inferred that increasing the steam to coal ratio renders cold gas efficiency to decrease due to decrease in CO and H_2 composition in the product gas. The increase in mole percentages of the CO_2 can be attributed to the fact that as the partial pressure of steam increases in water-gas shift reaction (5) at lower temperatures, carbon monoxide combines with steam to form CO_2 and hydrogen, that is, the rate of forward reaction increases making more CO_2 in the product gas. Increasing the steam to coal ratio promotes the gasification reaction but at the same time lowers the gasifier temperature significantly due to endothermic nature of gasification reaction. The heat absorbed by steam increases as steam to coal ratio increases, thereby, reducing the gasifier temperature. The reaction (4) is exothermic in nature and is very slow when the hydrogen partial pressure and temperature are low [10], but as the hydrogen composition increases with steam rate, the rate of methane formation becomes appreciable.

4.2. Effect of Oxygen to Coal Ratio. Oxygen plays an important role in coal gasification by increasing the efficiency of the gasifier and downstream processes [4]. Increasing the oxygen rate in the gasifier results in further oxidation of the char, which increases the temperature inside the gasifier. Figure 3 shows the variation in gasifier temperature with oxygen to coal ratio. Increase in gasifier temperature, in turn, enhances the endothermic steam-gasification reaction. Note that traditional nonslagging moving bed gasifiers will be temperature limited in operation as they have to be operated below the ash softening temperature, that is, the oxygen flow rate can only be increased up to a certain point. As a matter of information, the ash softening temperature for Usibelli coal is 1217°C, which is exceeded in the simulations when the oxygen-coal ratio reaches 0.26. Slagging moving bed gasifiers, of course, have no such limitations.

Figure 4 shows how the product gas composition changes with oxygen to coal ratio. The yield of CO increases

Table 2: Descriptions of the various reactor blocks used in the model.

Process	Reactor block used	Description
Coal drying	RYield	Simulates coal drying by considering the moisture content in the proximate analysis of the coal. RYield reactor block is used when both the stoichiometry and kinetics data of the reaction are unknown.
Coal pyrolysis	RYield	Simulates the coal pyrolysis process. Here, we specify the yield of the pyrolysis product using RYield reactor model.
Char decomposition	RStoic	Char decomposition is carried out in RStoic reactor block. RStoic block is used when the stoichiometry of the reaction is known, but kinetics data is unknown. RStoic block decomposes char into its constituents based on its ultimate analysis.
Char gasification and combustion	RCSTR	Simulates char gasification and combustion. Unlike the RYield and RStoic models, RCSTR block needs kinetics data for the reactions occurring in the reactor. Reactor volume, temperature, and reaction rates for all the reactions occurring in the reactor are required information.

Table 3: Proximate and ultimate analysis of the Usibelli coal [1].

Proximate analysis	As received %
Moisture	27
Fixed carbon	29
Volatile matter	36
Ash	8
Total	100.0
Ultimate analysis	DAF %
Carbon	69.5
Hydrogen	4.5
Nitrogen	0.9
Chlorine	—
Oxygen	24.8
Sulfur	0.3
Total	100.0
Heating value	18143 KJ/Kg

Table 4: Simulation model operational parameters.

Operational parameters for simulation	
Reactor pressure (KN/m^2)	2473.15
Bed diameter (m)	3.048
Bed height (m)	3.048
Bed voidage (m)	0.122
Coal feed rate (kg/hr)	6159.78
Steam feed rate (kg/hr)	6201.97
Oxygen feed rate (kg/hr)	1513.18
Heat transfer coefficient, W/m^{2}K	170.34
Maximum temperature attained, °C	1182

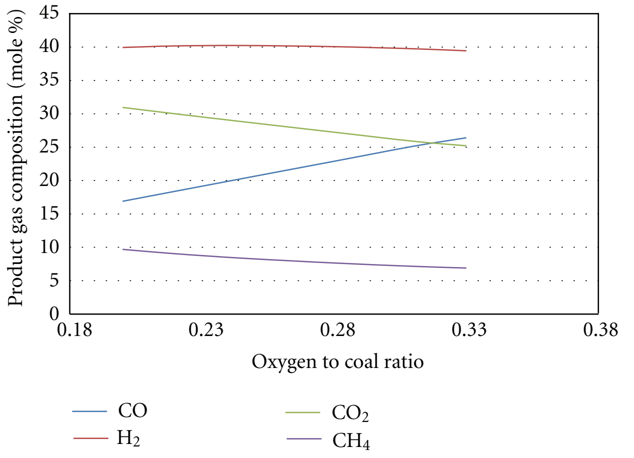

Figure 4: Effect of oxygen to coal ratio on product gas composition.

exponentially while CO_2 and CH_4 content decreases with the increase in oxygen to coal ratio. H_2 composition does not show any variation with the increase in oxygen in the gasifier. Increase in CO and decrease in CO_2 content can be explained by Le Chateliers's principle that the increase in temperature shifts the equilibrium to the reactant side for the water-gas shift reaction favoring the production of CO and steam. Boudouard reaction is faster at higher temperature, thereby, making more CO and less CO_2 in the product gas. As H_2 produced in the endothermic gasification reaction is counterbalanced by reverse water-gas shift reaction, there is very little change in H_2 content in the product gas. At higher temperature, rate of methanation reaction becomes appreciable, but methane production is also less due to no variation in hydrogen partial pressure.

4.3. Effect of Pressure. Operating gasifier at higher pressure has several advantages including reduction in the overall size of the gasifier and the elimination of the expensive step of synthesis gas compression in the production of synthesis chemicals. The pressure in the gasifier is usually selected in accordance with the end use of the syngas. That is, whether it will be used for power generation, chemical synthesis, and so forth, Figure 5 shows the impact of pressure on the product gas composition. With the increase in pressure from 1 atm to 25 atm, H_2 content increased from 37.9% to 40.3%; CO content decreased from 22.58% to 20.3%, while CH_4 content remained unchanged. The CH_4 content remained the same probably because the pyrolysis model did not consider

Table 5: Comparing product gas composition of model with experimental data.

Component	CO	H_2	CO_2	CH_4	H_2S	N_2	Tar
Experimental results [10], mole%	20.2	36.4	28.7	13	0.4	1.3	270.8 (kg/hr)
Simulation results, mole%	20.3	40.2	28.8	8.4	0.2	1.13	114.21 (Kg/hr)

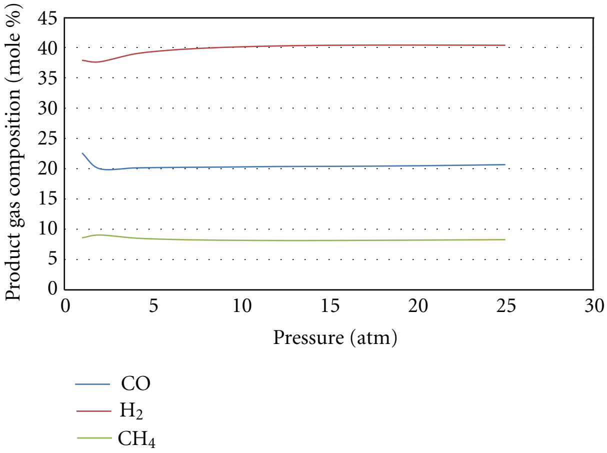

Figure 5: Effect of pressure on product gas composition.

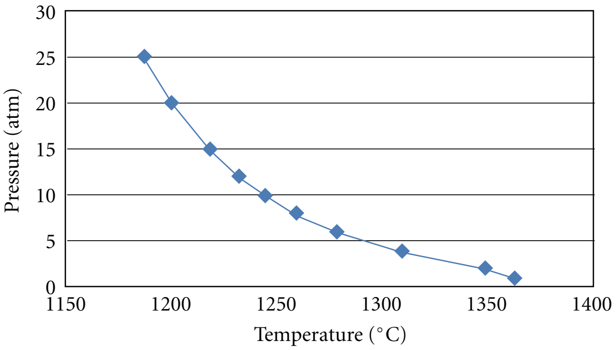

Figure 6: Effect of pressure on gasifier temperature.

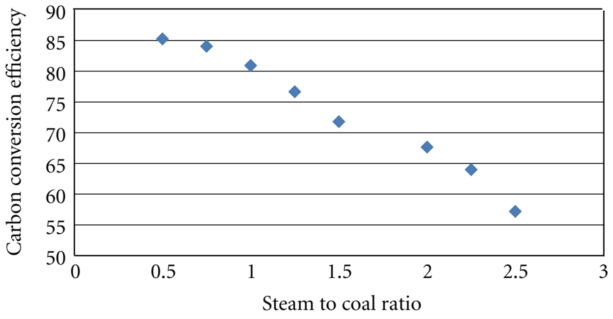

Figure 7: Carbon conversion efficiency (%) versus steam to coal ratio.

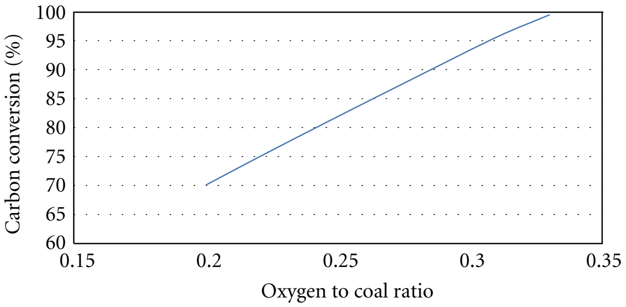

Figure 8: Effect of oxygen to coal ratio on carbon conversion.

pressure. Although synthesis gas composition altered during the pressure change, the variation is very small. This is consistent with the finding that pressure impacts the location of the temperature peak within the reactor, rather than the magnitude of the peak [15]. As noted earlier, temperature impacts product gas composition. The location of the peak indicates the location of combustion zone within the reactor [4]. Figure 6 shows variation in gasifier temperature with pressure. Although temperature showed increasing trend with decreasing pressure, temperature increase did not substantially altered the product gas composition.

4.3.1. Carbon Conversion Efficiency. Carbon conversion efficiency is defined here as the proportion of carbon in feedstock that is converted into gaseous products.

Figure 7 shows the effect of steam to coal ratio on carbon conversion efficiency. Steam to coal ratio has been varied from 0.75 to 2.5 at a constant oxygen rate of 1513.18 kg/hr. The maximum carbon conversion efficiency of 85.3% was achieved when steam to coal ratio was 0.5. It is obvious from Figure 5 that the carbon conversion efficiency shows decreasing trend with the increase in steam to coal ratio. The higher steam rate decreases the gasifier temperature [4, 16] and moves the peak temperature zone downwards [14], both of which leach to less conversion of carbon [4, 16].

Figure 8 shows the impact of oxygen to coal ratio on carbon conversion. Steam rate was kept constant at 6201.97 kg/hr to investigate the effect of oxygen to coal ratio on carbon conversion. On varying oxygen to coal ratio (0.2 to 0.33), it was found that the increase in oxygen rate increased the carbon conversion significantly. The increase in oxygen rate enhances the oxidation reactions, leading to higher amount of conversion of carbon to gaseous molecules. Carbon conversion efficiency of 99.5% was achieved when the oxygen to coal ratio was 0.33.

5. Conclusion

Although gasification is considered to be a well-proven, energy efficient and environmental friendly technology, the research on this technology is very limited for Alaska coal.

Moving bed gasifier technology is considered in this work due to its suitability for low-rank coal, higher thermal efficiency, and limited use of expensive oxygen. The main objective of this work was to get an insight into the performance of Usibelli coal in a moving bed gasifier. The overall process was modeled using Aspen Plus process simulator. The simulation results were validated by comparing it with the experimental results and showed reasonable agreements with the product gas compositions. The simulations were used to study the effect of steam to coal ratio, oxygen to coal ratio, and pressure on the product gas composition and carbon conversion efficiency. Results reveal that steam to coal ratio and oxygen to coal are the governing factor controlling both carbon conversion and product gas composition. An increase in oxygen to coal ratio led to an increase in carbon conversion significantly. Oxygen to coal ratio of 0.33 is necessary in order to get carbon conversion of 99.5%. Although synthesis gas showed decreasing trend with increasing pressure, this variation was almost insignificant. The results obtained through simulations are encouraging and can be useful for designing medium to large-sized moving bed gasifier using Usibelli coal.

Nomenclature

b: The correction factor taking into account the relative reactivity of ash to the iron-baseed catalyst
$[C]$: Concentration of char, g-mole/cm^3
C_{ps}: Heat capacity of the coal, cal/g$\cdot{}^\circ$K
d_p: Coal particle diameter, cm
E_i: Activation energy for the reaction (i), cal/g-mole
F: Geometric factor related with radiation heat transfer
hc: Convective heat transfer coefficient, cal/cm$^2\cdot{}^\circ$K$\cdot$sec
H_i: Heat of reaction i, cal/g-mol
k_{ash}: Mass transfer coefficient for ash diffusion, g/cm$^2\cdot$atm$\cdot$s.
k_{film}: Mass transfer coefficient for gas film diffusion, g/cm$^2\cdot$atm$\cdot$s.
k_2: Reaction rate coefficient for reaction (2), 1/atm$\cdot$sec
k_s: Chemical reaction constant, g/cm$^2\cdot$atm$\cdot$s.
k_{wgs}: The equilibrium constant for water gas shift reaction
k_3: Reaction rate coefficient for reaction (3), 1/atm$\cdot$sec
P_i: Partial pressure of reactant i, atm
$P_i{}^*$: Back reaction equilibrium pressure of reactant i, atm
R_i: The reaction rate for reaction (i), g-mole/cm$^3\cdot$sec
X_i: Mole fraction of species i
T: Temperature, $^\circ$K
T_w: Temperature of the reactor wall, $^\circ$K
Y: Ratio of radius of unreacted core to the radius of feed coal particle
ρ_c: Density of coal, gm/cm^3
ε_p: Porosity of the ash
ε_{bed}: Porosity of the bed
σ: Stephan-Boltzman constant (cal/cm$^2\cdot{}^\circ$K$^4\cdot$sec).

Acknowledgments

The authors wish to thank the United States Air Force for sponsoring this research. The help of Professor Daniel Walsh in giving advice and providing access to the very useful reports from the Mineral Industry Research Laboratory (University of Alaska Fairbanks) is also kindly acknowledged.

References

[1] R. C. Johnson and R. M. Flores, "Developmental geology of coalbed methane from shallow to deep in Rocky Mountain basins and in Cook Inlet-Matanuska Basin, Alaska, USA and Canada," *International Journal of Coal Geology*, vol. 35, no. 1–4, pp. 241–282, 1998.

[2] R. Chaney and B. Sheets, "Beluga coal gasification feasibility study," DOE/NETL-1248, 2006.

[3] L. Bibber, C. Thomas, and R. Chaney, "Alaskan coal gasification feasibility studies-healy coal-to-liquid plant," DOE/NETL/1251, 2007.

[4] H. Yoon, J. Wei, and M. M. Denn, "A model for moving bed coal gasification reactors," *AIChE Journal*, vol. 24, no. 5, pp. 885–903, 1978.

[5] P. R. Solomon, D. G. Hamblen, R. M. Carangelo, M. A. Serio, and G. V. Deshpande, "General model of coal devolatilization," *Energy and Fuels*, vol. 2, no. 4, pp. 405–422, 1988.

[6] T. H. Fletcher, A. R. Kerstein, R. J. Pugmire, M. S. Solum, and D. M. Grant, "Chemical percolation model for devolatilization. 3. Direct use of ^{13}C NMR data to predict effects of coal type," *Energy and Fuels*, vol. 6, no. 4, pp. 414–431, 1992.

[7] E. M. Suuberg, W. A. Peters, and J. B. Howard, "Product composition and kinetics of lignite pyrolysis," *Industrial and Engineering Chemistry Process Design and Development*, vol. 17, no. 1, pp. 37–46, 1978.

[8] J. Gibbins-Matham and R. Kandiyoti, "Coal pyrolysis yields from fast and slow heating in a wire-mesh apparatus with a gas sweep," *Energy and Fuels*, vol. 2, no. 4, pp. 505–511, 1988.

[9] H. E. Nuttall, W. G. Stoddard, and R. Chen, "Pyrolysis of Sub-bituminous New Mexico coal," *SPE Journal of Petroleum Technology*, vol. 31, no. 4, pp. 418–420, 1979.

[10] Wen, H. Chen, and M. Onozaki, "User's Manual for Computer Simulation and Design of the Moving-Bed Coal Gasifier, Final Report," DOE/MC/16474-1390, 1982.

[11] J. S. Kasule, R. Turton, D. Bhattacharya, and S. E. Zitney, "Mathematical modeling of a single-stage, downward firing, entrained flow gasifier," *Industrial and Engineering Chemistry Research*, vol. 51, no. 18, pp. 6429–6440, 2012.

[12] Aspen Tech, "ASPEN plus model for moving bed gasifier," 2010.

[13] P. D. Rao and D. E. Walsh, "Characterization of coal properties from high temperature processing of Usibelli Low Rank coal," MIRL Report 92, 1991.

[14] C. Higman and M. Vander Burgt, "Gasification," 2003.

[15] G. J. Stiegel and M. Ramezan, "Hydrogen from coal gasification: an economical pathway to a sustainable energy future," *International Journal of Coal Geology*, vol. 65, no. 3-4, pp. 173–190, 2006.

[16] M. L. Hobbs, P. T. Radulovic, and D. L. Smoot, "Modeling fixed-bed coal gasifiers," *AIChE Journal*, vol. 38, no. 5, pp. 681–702, 1992.


Journal of
Engineering


The Scientific World Journal


International Journal of
Rotating Machinery


Journal of
Sensors


International Journal of
Distributed Sensor Networks

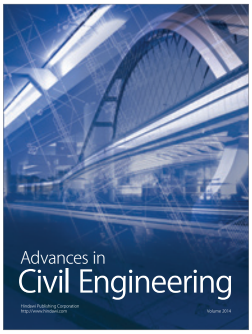
Advances in
Civil Engineering

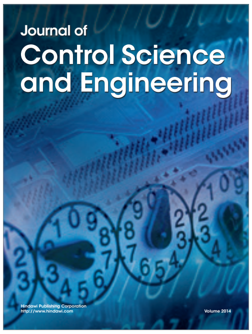
Journal of
Control Science and Engineering


Journal of
Robotics


Journal of
Electrical and Computer Engineering

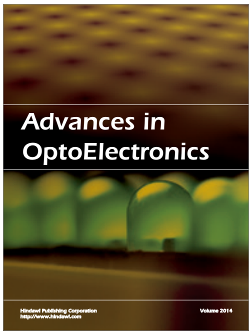
Advances in
OptoElectronics


VLSI Design


International Journal of
Navigation and Observation

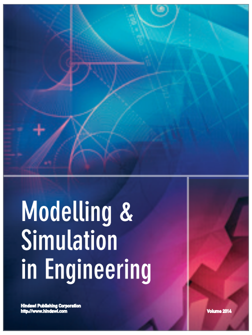
Modelling & Simulation in Engineering


International Journal of
Aerospace Engineering

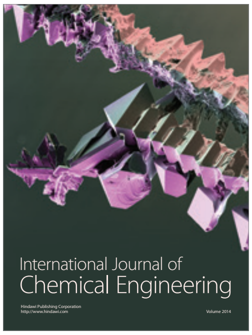
International Journal of
Chemical Engineering

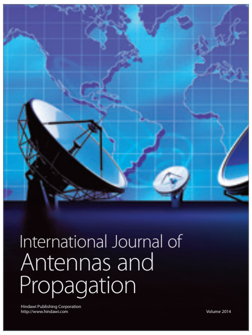
International Journal of
Antennas and Propagation


Active and Passive
Electronic Components

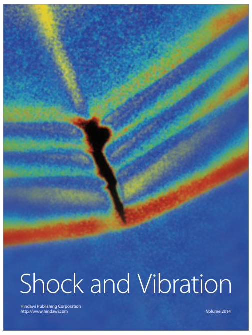
Shock and Vibration

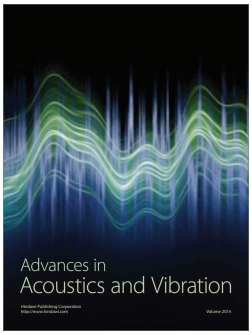
Advances in
Acoustics and Vibration